# 15A.7 RAPID-SCAN RADAR OBSERVATIONS OF $Z_{DR}$ COLUMN DEPTH AND ITS POTENTIAL USE DURING THE WARNING DECISION PROCESS

Charles M. Kuster*[1,2,3], Jeffrey C. Snyder[1,2,3], Terry J. Schuur[1,2,3], J. W. Brogden[1,2,3], R. Toomey[1,2,3], and Pamela L. Heinselman[2,3]

[1]Cooperative Institute for Mesoscale Meteorological Studies, [2]NOAA/OAR National Severe Storms Laboratory, [3]University of Oklahoma, Norman, Oklahoma

ABSTRACT

National Weather Service forecasters employ conceptual models during warning operations to help them anticipate threats posed by a given storm. The dual-polarization upgrade of the National Weather Service radar network may provide forecasters with additional information that could aid in severe weather warning decisions. This additional information will likely be more useful and used more if it can be incorporated into existing forecaster conceptual models. To aid this process, 15 rapid-update (1.6–2.1 min volumes) radar cases collected by a research Weather Surveillance Radar-1988 Doppler radar located in Norman, OK (KOUN) were analyzed. The $Z_{DR}$ column depth of 42 storms—ranging from supercells to multicells and severe storms to nonsevere storms—was compared to features forecasters typically use to issue severe-weather warnings (e.g., upper-level reflectivity cores, storm reports, etc.) to identify any operatically useful relationships. Analysis of all cases consisting of over 1400 volume scans has revealed that 1) no major differences exist between the $Z_{DR}$ column depth of tornadic and nontornadic storms, 2) significant differences do exist between the $Z_{DR}$ column depth of severe and nonsevere storms, 3) $Z_{DR}$ columns evolve prior to -20°C reflectivity cores and therefore provide additional time to anticipate changes in storm intensity and issue warnings, and 4) rapid-update radar data captures trends in $Z_{DR}$ column depth evolution up to 4 min earlier than traditional-update (about 5-min volumes) radar data, thereby providing forecasters with extra time to consider storm trends and issue warnings.

## 1. INTRODUCTION

In 2013, the dual-polarization (dual-pol) upgrade of the Weather Surveillance Radar-1988 Doppler (WSR-88D) radar network provided new opportunities for forecasters to assess thunderstorm organization and intensity through the introduction of additional radar variables and signatures (NOAA 2013). One such signature, known as the differential reflectivity column ($Z_{DR}$ column), can likely provide National Weather Service (NWS) forecasters with important information about the location and intensity of a storm's updraft (e.g., Ryzhkov et al. 1994; Kumjian et al. 2014; Snyder et al. 2015). Information about updrafts is important because an increase in updraft size or intensity can result in an increase in low-level rotation, hail size, and precipitation intensity (e.g., Nelson 1983; Picca and Ryzhkov 2012; Snyder et al. 2015). Changes in $Z_{DR}$ column magnitude may therefore precede these hazards and provide forecasters with an additional tool for anticipating storm-related threats (e.g., Kumjian and Ryzhkov 2008; Picca et al. 2010; Kumjian 2013).

Despite the growing body of knowledge related to dual-pol signatures, it remains unclear how $Z_{DR}$ columns can be explicitly used to make or support warning decisions (T. Lindley, Science Operation Officer at NWS Norman Forecast Office, 2017, personal communication) and multiple knowledge gaps still exist especially regarding $Z_{DR}$ columns of nontornadic supercells, impact of radar update time, and links to operational utility (e.g., Van Den Broeke et al. 2008; Picca et al. 2015; Van Den Broeke 2017). Therefore, the purpose of this study is to examine $Z_{DR}$ column evolution across multiple storm modes and intensities and then compare this evolution to features such as upper-level reflectivity cores, mesocyclones, and storm reports that forecasters typically use during the warning decision process. The ultimate goal is to link $Z_{DR}$ columns with existing forecaster conceptual models. We expect $Z_{DR}$ columns will be more useful and used more frequently to aid in warning decisions if they can be linked to what forecasters are already using to issue warnings.

*Corresponding author address: Charles M. Kuster, National Weather Center, 120 David L. Boren Blvd., Norman, OK, 73072. E-mail: charles.kuster@noaa.gov

## 2. RADAR DATA AND STORM INFORMATION

Over the past five years, a unique radar dataset has been built using a research WSR-88D located in Norman, OK (KOUN). Radar operators collected 90° sector scans and designed special volume coverage patterns (VCPs) that contained fewer elevation angles than traditional VCPs in order to collect volumetric data with update times of about 2 min or less. In total, we analyzed 49 different storms across 15 KOUN cases. Seven storms were unusable due $Z_{DR}$ column contamination (Section 3.6), so this paper will focus on analysis of 42 storms—ranging from severe supercells to nonsevere multicells—and over 1400 volume scans spanning 13 cases (Table 1).

Table 1. Sample size for each storm type in terms of number of storms and number of volume scans.

| Storm Type | # of Storms | # of Volume Scans |
|---|---|---|
| Supercell | 22 | 832 |
| Single Cell/Multicell | 20 | 587 |
| Severe | 25 | 934 |
| Nonsevere | 17 | 485 |
| Tornadic Supercell | 10 | 447 |
| Nontornadic Supercell | 12 | 395 |

For each case, two algorithms generated output for analysis. The $Z_{DR}$ column depth algorithm (Snyder et al. 2015) produces a grid of $Z_{DR}$ column depth above the environmental melting layer (Fig. 1a), while the w2merger algorithm contained within the Warning Decision Support System-Integrated Information software (Lakshmanan et al. 2007) produces a grid of reflectivity at -20°C (Fig. 1b). Both algorithms use the Rapid Refresh model (Brown et al. 2011) for environmental temperature information and output grids with a resolution of 0.0025° in latitude and longitude and 250 m in the vertical.

## 3. RADAR DATA ANALYSIS

To measure signature evolution, we manually extracted data from the $Z_{DR}$ column depth and -20°C reflectivity field and then calculated median and maximum values as well as signature size (i.e., spatial extent). To aid in separating individual signatures—especially in instances of widespread convection—and to ensure that results were operationally significant, we calculated the aforementioned signature metrics for $Z_{DR}$ column depth of 1000 m or higher and -20°C reflectivity of 50 dBZ or higher. To measure midlevel mesocyclone evolution, we calculated the velocity difference across the mesocyclone signature (DeltaV) at the elevation angle closest to 3 km above radar level. Using Mann-Whitney U tests (Mann and Whitney 1947), we then compared differences in these metrics between different storm modes (e.g., multicell vs. supercell) and storm intensities (e.g., severe vs. nonsevere) to examine operationally relevant applications of $Z_{DR}$ column depth.

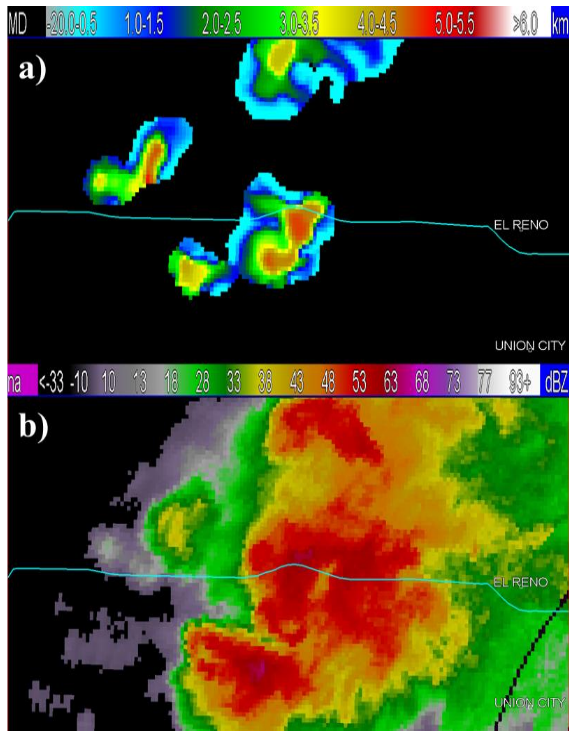


Fig. 1: Example of a) $Z_{DR}$ column depth and b) -20°C reflectivity. In a), warmer colors indicate greater $Z_{DR}$ column depth. Example uses data from the 31 May 2013 tornadic supercell near El Reno, Oklahoma.

### 3.1 $Z_{DR}$ COLUMNS OF TORNADIC AND NONTORNADIC STORMS

No operationally significant differences existed between the $Z_{DR}$ column depth or -20°C reflectivity of tornadic and nontornadic supercells or between tornadic and nontornadic mesocyclones. Statistically significant (i.e., $p < 0.005$) differences did exist for three radar metrics—median column depth, max column depth, and median -20°C reflectivity—pertaining to supercells (Fig. 2a) and one radar metric—median -20°C reflectivity—pertaining to mesocyclones (Fig. 2b), but there

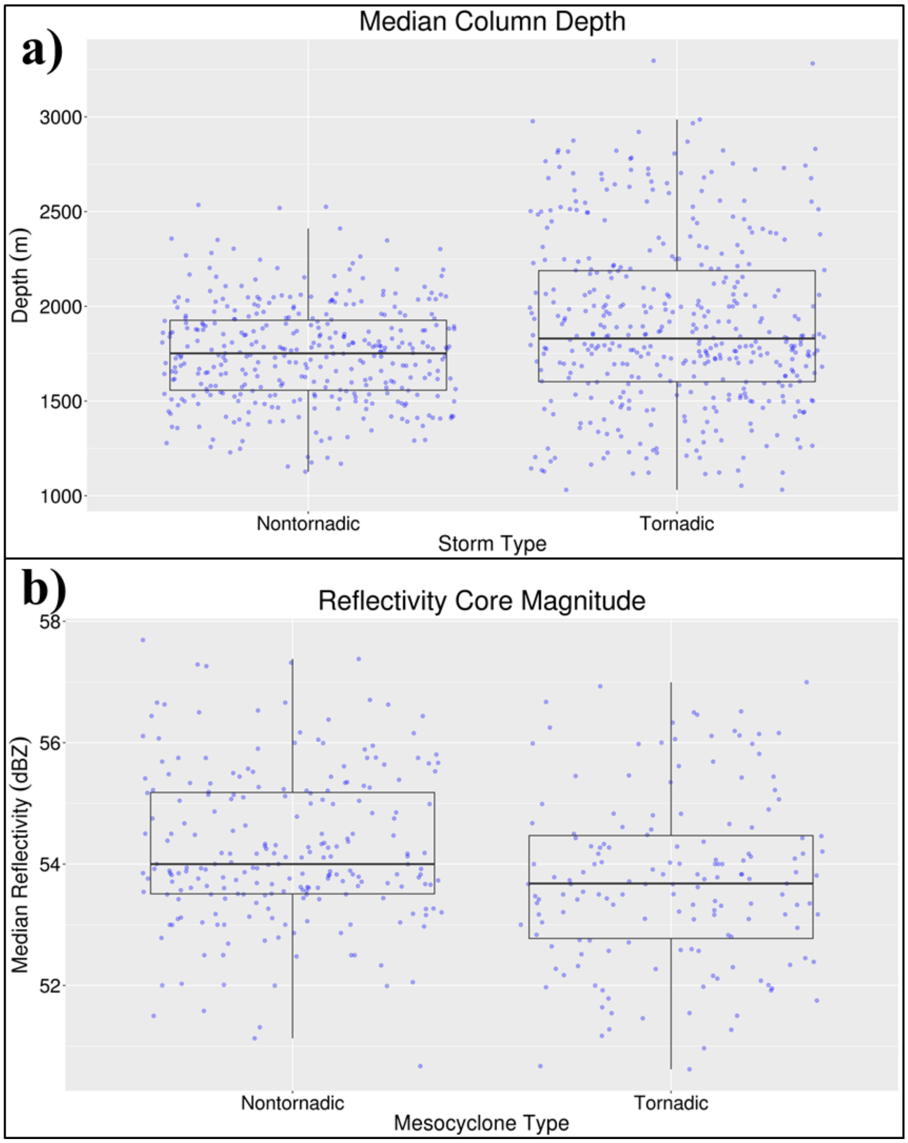


Fig. 2. Box and whisker plots showing distribution of a) median $Z_{DR}$ column depth between nontornadic and tornadic supercells and b) median reflectivity within the -20°C reflectivity core between nontornadic and tornadic mesocyclones. The middle black line indicates the median value, box edges indicate the lower and upper quartiles (i.e., interquartile range), and whiskers indicate the minimum and maximum values (excluding outliers). Blue dots show data from each individual volume scan used to create the plot.

was a lot of overlap between the distributions and it is likely forecasters could not effectively use $Z_{DR}$ column depth or -20°C reflectivity cores alone to make any decisions about a storm's tornadic potential, at least based on results from this sample of storms in Oklahoma. These results also corroborate results from previous studies (e.g., Picca et al. 2015; Van Den Broeke 2017)

### 3.2 $Z_{DR}$ COLUMNS OF SEVERE AND NONSEVERE STORMS

Statistically significant differences were observed between the $Z_{DR}$ columns and -20°C reflectivity cores of severe and nonsevere thunderstorms. Distributions of all radar metrics for both $Z_{DR}$ column depth and -20°C reflectivity had statistically significant differences. Signature size (i.e., $Z_{DR}$ column depth size and -20°C reflectivity core size) contained the most significant differences between severe and nonsevere storms (Fig. 3). It is therefore likely important for forecasters to pay special attention to changes in $Z_{DR}$ column and -20°C reflectivity core size while interrogating radar data since size differences may

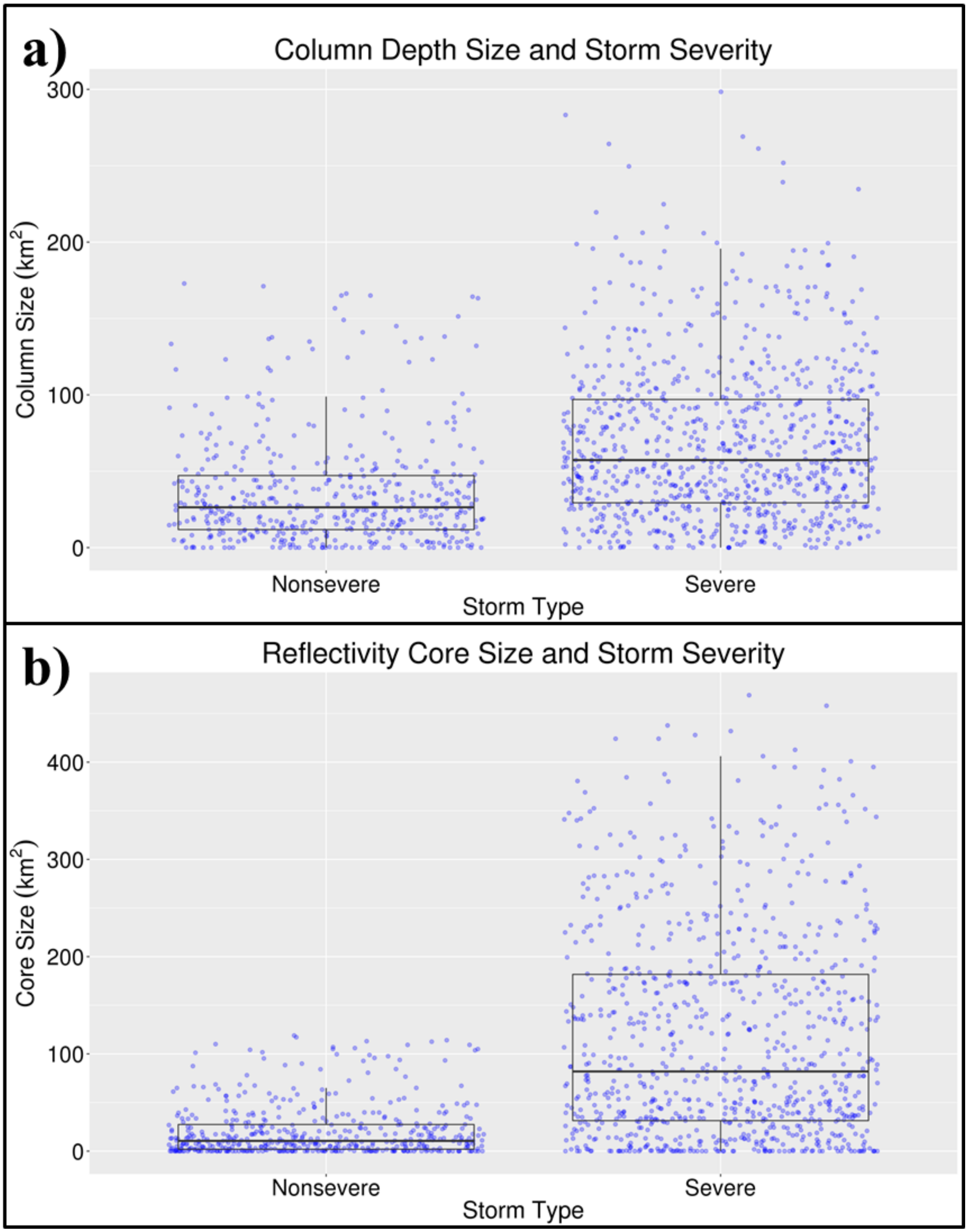


Fig. 3. As in Fig. 2 but for a) $Z_{DR}$ column depth size between nonsevere and severe thunderstorms (i.e., storms not associated with and associated with severe-weather reports in NCEI's Storm Data publication respectively), and b) -20°C reflectivity core size between nonsevere and severe thunderstorms.

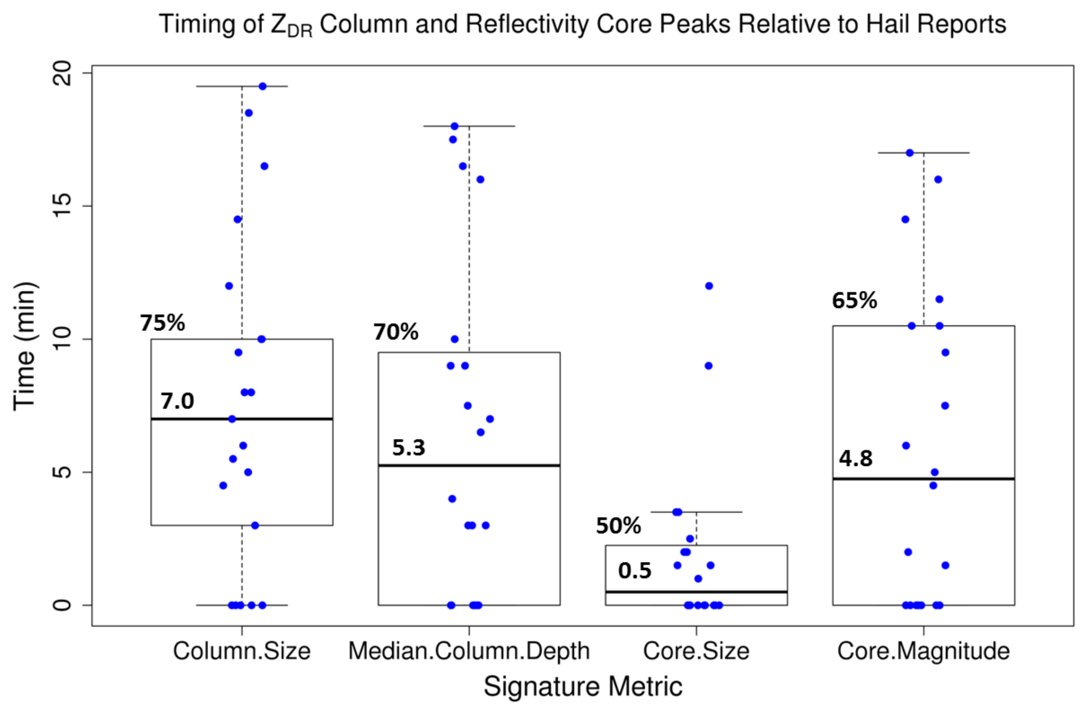


Fig. 4. Box and whisker plot showing timing of various radar metric peaks prior to severe hail reports. Median value and percentage of hail reports preceded by a peak in each signature metric are annotated. Blue dots indicate timing data for each hail report used to create the plot. Box and whisker convention is the same as in Fig. 2.

present the best discriminator between severe and nonsevere storms. It is also likely important to have automated algorithms that can calculate signature size in real time and produce time series plots for forecasters. These additional visualizations of radar data would likely help forecasters observe changes—especially subtle ones—in signature size more easily and more quickly than using radar imagery alone.

It is also important to note that the most statistically significant differences between radar metrics occurred with -20°C reflectivity rather than $Z_{DR}$ column depth (Fig 3). One focus of this research is to determine if $Z_{DR}$ columns provide useful information to forecasters in addition to the signatures forecasters are already using to issue warnings. These results suggest that $Z_{DR}$ column depth is no better at discriminating between severe and nonsevere storms than upper-level (e.g., -20°C) reflectivity cores. While there may not be additional benefits of $Z_{DR}$ columns relative to storm intensity, there do appear to be additional benefits relative to the timing of $Z_{DR}$ columns compared to -20°C reflectivity cores.

### 3.3 $Z_{DR}$ COLUMNS EVOLVE PRIOR TO UPPER-LEVEL REFLECTIVITY CORES

$Z_{DR}$ column depth typically increased and reached its peak magnitude prior to -20°C reflectivity cores in the analyzed storms. In 30 out of the 42 storms (71%), the first peak in $Z_{DR}$ column depth size occurred before the first peak in -20°C reflectivity core size. It was also common for subsequent peaks in signature size to evolve in a similar manner, with the $Z_{DR}$ column depth peak occurring before the -20°C reflectivity core peak. Previous research (e.g., Knight 2006, Snyder et al. 2015; Carlin et al. 2017; Kuster et al. 2017) has also noted this earlier evolution of $Z_{DR}$ columns and suggests that it occurs due to size sorting within the updraft in addition to the $Z_{DR}$ column occurring at an altitude below the altitude of maximum updraft magnitude. While this result is not surprising, it is important for forecasters to consider during warning operations, because it could provide them with additional time to anticipate changes in storm intensity and therefore may help them issue warnings with slightly longer lead time.

The potential benefits offered by the earlier evolution of $Z_{DR}$ column depth was also observed when examining a subset of data related to 21 severe hail reports associated with the analyzed storms. Peaks in $Z_{DR}$ column depth size occurred about 7.0 min (median value) prior to hail reports in this study, while peaks in -20°C reflectivity core size occurred about 0.5 min (median value) prior to hail reports (Fig. 4). Peaks in $Z_{DR}$ column depth size occurred on average 5.5 min prior to peaks in -20°C reflectivity core size and as much as 18.5 min prior. Additionally, 75% percent of hail reports were preceded by a peak in $Z_{DR}$ column depth size while 50% of hail reports were preceded by a peak in -20°C reflectivity core size (Fig. 4). The difference in lead times and occurrence rates between peaks in $Z_{DR}$ column depth magnitude and -20°C reflectivity core magnitude were much less than differences between signature size. It is also important to note that while -20°C reflectivity core size provided the best discriminator between severe and nonsevere storms, it also provided the shortest amount of time between signature peak and hail report. Therefore, due to the earlier timing, frequent occurrence prior to hail reports, and good discrimination between severe and nonsevere storms (Section 3.2), it is likely that monitoring $Z_{DR}$ column depth evolution will be beneficial for forecasters during the warning decision process.

### 3.4 $Z_{DR}$ COLUMN RELATIONSHIP TO CURRENLTY USED RADAR SIGNATURES

Since $Z_{DR}$ column depth could provide beneficial information to forecasters, linking $Z_{DR}$ column depth evolution to the evolution of signatures that forecasters currently use to issue warnings will likely help forecasters integrate this information into their existing conceptual models more easily. We therefore examined relationships between $Z_{DR}$ column depth and -20°C reflectivity cores and 3-km mesocyclone intensity. No strong relationships were found between the signatures (Fig. 5) at least when comparing them at the same volume scan (i.e., same time). While we did not expect a relationship to exist between $Z_{DR}$ column depth and mesocyclone intensity (Section 3.1; Van Den Broeke 2017), we did expect to observe a relationship between $Z_{DR}$ column depth and -20°C reflectivity cores. We suspect that the lack of a relationship may be due at least in part to the fact that $Z_{DR}$ columns evolve earlier than -20°C reflectivity cores (Section 3.3). A comparison of these signatures at varying time lags (i.e., lag correlations) may provide more insight into signature relationships.

### 3.5 IMPACT OF RADAR UPDATE TIME

To explore the potential impacts of volumetric radar update times on sampling signatures such as $Z_{DR}$ columns, we compared rapid-update KOUN data to data collected by a nearby WSR-88D (KTLX) with volume update times typically near five minutes. For the considered storms, rapid-update data sampled changing trends in $Z_{DR}$ column depth up to 4 min before conventional-update data. The additional time afforded by the rapid-update data depended on the spacing of the KTLX volume scans relative to changes in $Z_{DR}$ column trends. This idea is exemplified by the $Z_{DR}$ column depth size evolution of a supercell that occurred on 31 May 2013 (Fig. 6). At about 2214:27 UTC, a forecaster using KTLX data would see a decreasing trend in the $Z_{DR}$ column depth size. By the next volume scan—about 4.5 min later at 2219:20 UTC—the forecaster would then see an increasing trend that then continues for the next few volume scans. A forecaster using rapid-update data from KOUN could see an increasing trend in $Z_{DR}$ column depth size as early as 2216:28 UTC or about 3 min earlier than that seen in the KTLX data. Later, after the first substantial peak, a forecaster using KOUN data might see a decreasing trend in $Z_{DR}$ column depth size beginning at about 2238:01 to 2239:40 UTC. In this case, KTLX volume scans were spaced fortuitously, and a forecaster using this data could observe the decreasing trend at about the same time (2237:46 UTC) as a forecaster using KOUN data. The benefits of rapid-update data would also likely be slightly greater with a future dual-pol phased array radar system that could collect volume scans in 1 min or less as opposed to the 1.6–2.1 min volume scans collected by KOUN. Any additional time provided to forecasters by rapid-update data could be helpful because it would give forecasters more time to process observed trends and therefore have more time and data to anticipate upcoming changes in storm intensity, related hazards, and issue warnings more quickly (T. Lindley, Science Operation Officer at NWS Norman Forecast Office, 2017, personal communication).

### 3.6 OPERATIONAL LIMIATIONS

Analysis of these 15 cases revealed some limitations for using $Z_{DR}$ column depth in an operational setting. The biggest limitation related to $Z_{DR}$ column contamination due to the colocation of either hail or lofted tornadic debris with the $Z_{DR}$

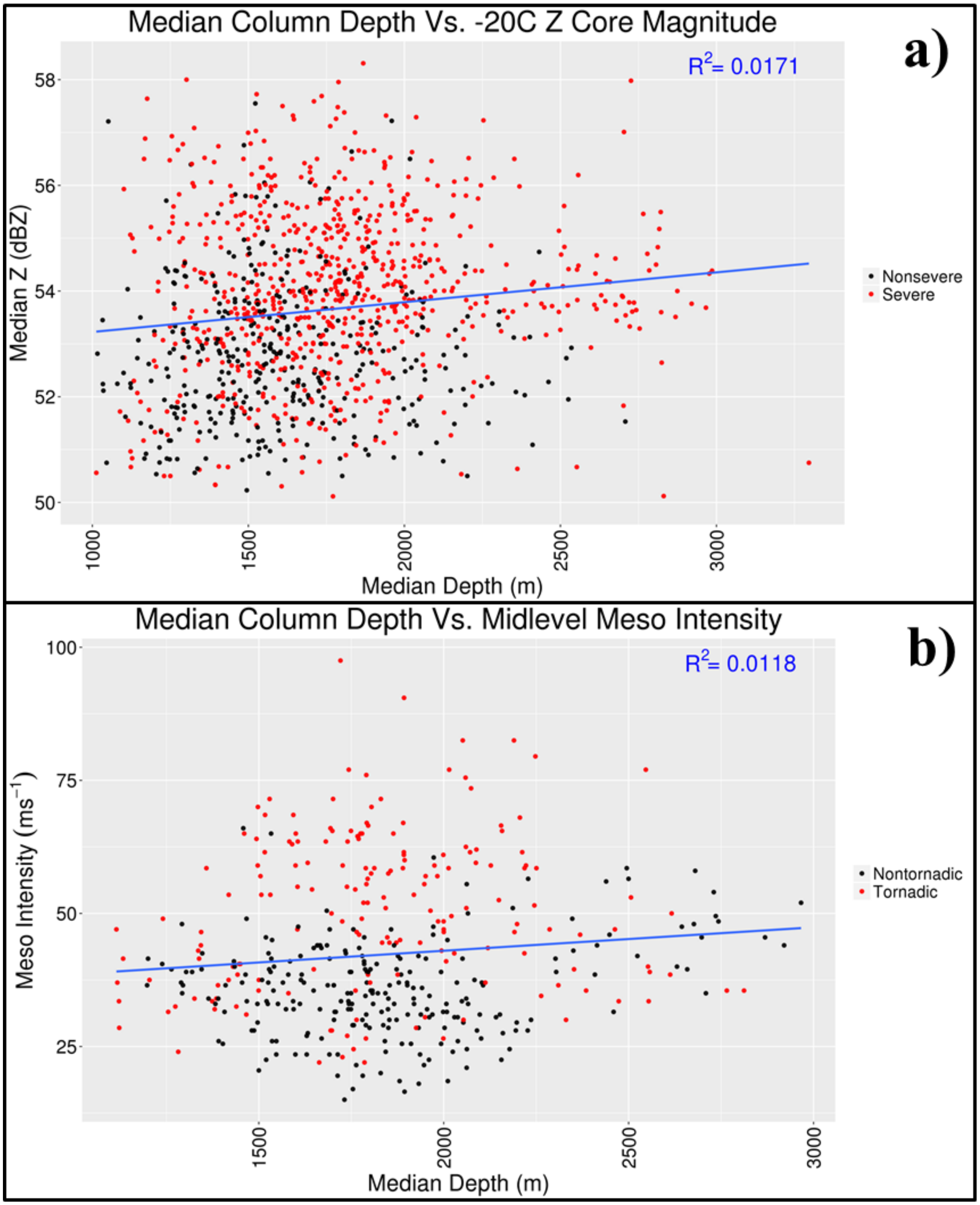

Fig. 5. Scatter plot showing distribution of a) median $Z_{DR}$ column depth relative to median reflectivity within the -20°C reflectivity core and b) median $Z_{DR}$ column depth relative to midlevel (3 km above radar level) mesocyclone intensity (DeltaV). Black dots indicate data of individual volume scans associated with nonsevere thunderstorms in a) and nontornadic mesocyclones in b). Red dots indicate data of individual volume scans associated with severe thunderstorms in a) and tornadic mesocyclones in b). Linear trend line and r-squared value is annotated in blue.

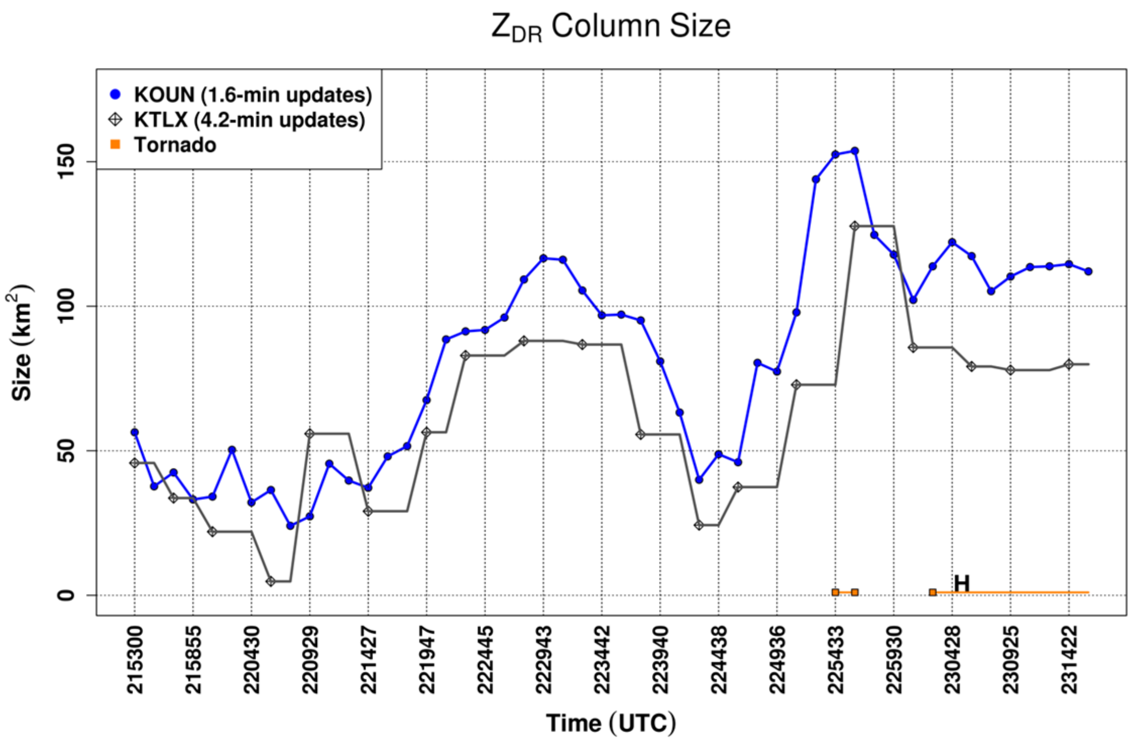


Fig. 6. Time series of $Z_{DR}$ column depth size for rapid-update KOUN data (blue line) and traditional-update KTLX data (grey line) for a tornadic supercell on 31 May 2013. Horizontal orange line indicates when a tornado was ongoing and the boldface letter "H" marks hail report time.

column. These large scatterers dominate the size-weighted $Z_{DR}$ field and therefore mask out smaller rain drops and wet hail that make up a $Z_{DR}$ column signature. We especially noticed this effect in prolific hail-producing thunderstorms that had large high reflectivity cores and significant three-body scatter spikes—which can also interfere with (i.e., contaminate) $Z_{DR}$ columns (Fig. 7). This contamination occurred in 7 out of the 49 storms (14%) we considered. While not common, forecasters would need to be aware that $Z_{DR}$ column evolution may not be observable especially in environments where widespread large hail is likely. Peaks in $Z_{DR}$ column depth size, median value, and maximum value were also quite common and many peaks did not precede severe weather at the surface. Future work aims to determine what peak values of $Z_{DR}$ column depth are significant and could alert forecasters to a storm's severe-weather potential, but forecasters should remain aware that the potential exists for false alarm peaks.

## 4. SUMMARY

$Z_{DR}$ column depth evolution does appear to offer operational utility especially with regards to anticipating changes in -20°C reflectivity cores and providing additional lead time for severe hail reports. Statistically significant differences existed between the $Z_{DR}$ column depth of severe and nonsevere storms. These differences were less than differences between the -20°C reflectivity cores of severe and nonsevere storms, but $Z_{DR}$ column depth typically changed prior to changes in the -20°C reflectivity cores, which could give forecasters additional time to anticipate storm evolution and make warning decisions (Section 3.3). This difference in timing may also explain why no strong relationships were observed between $Z_{DR}$ column depth and -20°C reflectivity cores. Lag correlations will be examined in the future to further explore any relationships between these signatures. Rapid-update radar data (1–2 min volumes) can also provide additional time to forecasters for making decisions because rapid-scan radars can sample changes in $Z_{DR}$ column depth trends up to 4 min earlier than traditionally-scanning WSR-88Ds. This effect would be maximized with the use of a dual-pol phased array radar system that could scan more rapidly than the research WSR-88D used in this study. Further lead time benefits of rapid-update radars would also occur when compared to WSR-88Ds utilizing Supplemental Adaptive Intravolume Low-Level

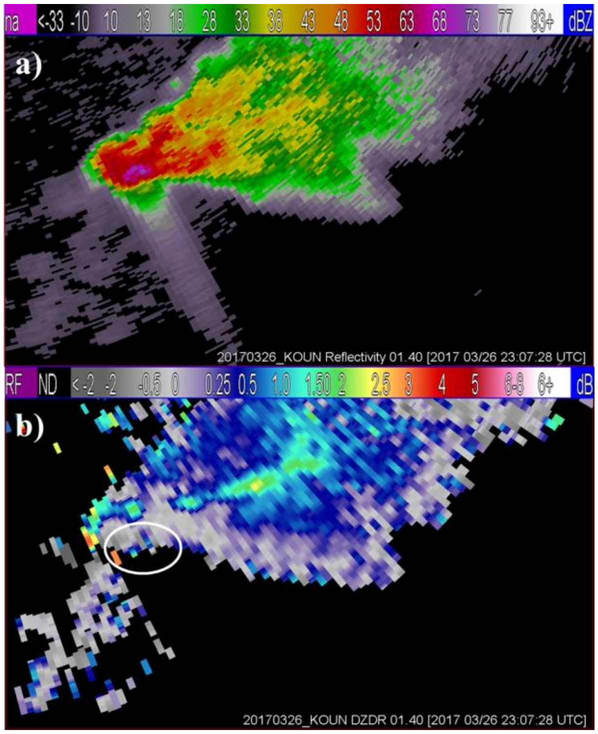


Fig. 7. 1.4° (about 2.2 km above radar level) plan position indicator from 26 March 2013 of a) reflectivity and b) $Z_{DR}$ showing $Z_{DR}$ column contamination caused by a hail-filled high-reflectivity core and three-body scatter spike. White circle in b) indicates one approximate area where $Z_{DR}$ column might be expected but is not evident.

Scans (SAILS; Crum et al. 2013) because SAILS slows down volumetric update times and would therefore negatively impact the ability to sample rapid changes in $Z_{DR}$ columns.

One important area of future research for operational use of $Z_{DR}$ columns is determining what information (if any) $Z_{DR}$ columns can provide about hail size. If there were differences in the $Z_{DR}$ column depth evolution between storms that produced significant hail (2 inches in diameter or greater) and those that did not, forecasters could gain valuable insight into the potential impacts and danger posed by a given storm. Additionally, if there were a value of $Z_{DR}$ column depth that could alert forecasters that a warning may be needed—similar to current reflectivity-at-height thresholds used now (i.e., height of 50 dBZ isosurface; e.g., Lemon 1977, 1978; Donavon and Jungbluth 2007)—it could allow forecasters to issue severe thunderstorm warnings with somewhat higher lead time since $Z_{DR}$ columns develop and evolve prior to upper-level reflectivity cores. Answering both of these future research questions will likely require a large sample size (much larger than this study) of $Z_{DR}$ column depth information collected by radars across the country.

*Acknowledgements.* We thank John Krause for help with Perl programming, Eddie Forren for KOUN data processing, Danny Wasielewski, Micheal Shattuck, Allen Zahrai, and Rafael Mendoza for KOUN data collection support, Karen Cooper for help with WDSS-II, Katie Wilson for research insights, Tanya Riley and Tracy Reinke for help with travel and administrative logistics, and six NWS Norman Forecast Office employees (Ryan Barnes, Randy Bowers, Todd Lindley, Vivek Mahale, Richard Smith, and Doug Speheger) for providing operational guidance on radar data analysis. Funding for CK, JS, TS, JB, and RT was provided by NOAA/Office of Oceanic and Atmospheric Research under NOAA-University of Oklahoma Cooperative Agreement #NA11OAR4320072, U.S. Department of Commerce.

**REFERENCES**

Brown, J. M., and Coauthors, 2011: Improvement and testing of WRF physics options for application to Rapid Refresh and High Resolution Rapid Refresh. *Proc. 14th Conf. on Mesoscale Processes/15th Conf. on Aviation, Range, and Aerospace Meteorology*, Los Angeles, CA, Amer. Meteor. Soc., 5.5. [Available online at https://ams.confex.com/ams/14Meso15ARAM/webprogram/Paper191234.html.]

Carlin, J. T., J. Gao, J. C. Snyder, and A. V. Ryzhkov, 2017: Assimilation of $Z_{DR}$ columns for improving the spinup and forecast of convective storms in storm-scale models: Proof-of-concept experiments. *Mon. Wea. Rev.*, **145**, 5033–5057.

Crum, T. D., S. D. Smith, J. N. Chrisman, R. E. Saffle, R. W. Hall, and R. J. Vogt, 2013: WSR-88D radar projects – Update 2013. *Proc. 29th Conf. Environmental Information Processing Technologies*, Austin, TX, Amer. Meteor. Soc., 8.1. [Available online at https://ams.confex.com/ams/93Annual/webprogram/Paper221461.html.]

Donavon, R. A., and K. A. Jungbluth, 2007: Evaluation of a technique for radar identification of large hail across the Upper Midwest and central plains of the United States. *Wea. Forecasting*, **22**, 244–254.

Knight, C. A., 2006: Very early formation of big, liquid drops revealed by $Z_{DR}$ in continental cumulus. *J. Atmos. Sci.*, **63**, 1939–1953.

Kumjian, M. R., 2013: Principles and applications of dual-polarization weather radar. Part II: Warm- and cold-season applications. *J. Operational Meteor.*, **1**, 243–264.

——, and A. V. Ryzhkov, 2008: Polarimetric signatures in supercell thunderstorms. *J. Appl. Meteor. Climatol.*, **47**, 1940–1961.

——, A. P. Khain, N. Benmoshe, E. Ilotoviz, A. V. Ryzhkov, and V. T. Phillips, 2014: The anatomy and physics of $Z_{DR}$ columns: Investigating a polarimetric radar signature with a spectral bin microphysical model. *J. Appl. Meteor. Climatol.*, **53**, 1820–1843.

Kuster, C. M., J. C. Snyder, P. L. Heinselman, and T. J. Schuur, 2017: Rapid-scan dual-polarization radar observations of $Z_{DR}$ column depth in the context of forecaster conceptual models. *Extended Abstracts, 38th Conf. on Radar Meteorology*, Chicago, IL, Amer. Meteor. Soc., 19A.5. [Available online at https://ams.confex.com/ams/38RADAR/meetingapp.cgi/Paper/320591].

Lakshmanan, V., T. Smoth, G. J. Stumpf, and K. Hondl, 2007: The Warning Decision Support System-Integrated Information. *Wea. Forecasting*, **22**, 596–612.

Lemon, L. R., 1977: New severe thunderstorm radar identification techniques and warning criteria: A preliminary report. NOAA Tech. Memo. NWS NSSFC-1, 60 pp. [Available online at http://www.dtic.mil/dtic/tr/fulltext/u2/a099510.pdf].

——, 1978: On the use of storm structure for hail identification. Preprints, *18th Conf. on Radar Meteorology*, Atlanta, GA, Amer. Meteor. Soc., 203–206.

Mann, H. B., and D. R. Whitney, 1947: On a test of whether one of two random variables is stochastically larger than the other. *The Annals of Mathematical Statistics*, **18**, 50–60.

Nelson, S. P., 1983: The influence of storm flow structure on hail growth. *J. Atmos. Sci.*, **40**, 1965–1983.

NOAA 2013: Dual-polarization radar: Stepping stones to building a Weather-Ready Nation. Accessed 1 May 2018. [Available online at http://www.noaanews.noaa.gov/stories2013/20130425_dualpol.html].

Picca, J. C., and A. V. Ryzhkov, 2012: A dual-wavelength polarimetric analysis of the 16 May 2010 Oklahoma City extreme hailstorm. *Mon. Wea. Rev.*, **140**, 1385–1403.

——, M. Kumjian, and A. V. Ryzhkov, 2010: $Z_{DR}$ columns as a predictive tool for hail growth and storm evolution. *Extended Abstracts, 25th Conf. on Severe Local Storms*, Denver, CO, Amer. Meteor. Soc., 11.3 [Available online at https://ams.confex.com/ams/pdfpapers/175750.pdf].

——, J. C. Snyder, and A. V. Ryzhkov, 2015: An observational analysis of $Z_{DR}$ column trends in tornadic supercells. *Extended Abstracts, 37th Conf. on Radar Meteorology*, Norman, OK, Amer. Meteor. Soc., 5A.5. [Available online at https://ams.confex.com/ams/37RADAR/webprogram/Paper275416.html].

Ryzhkov, A. V., V. B. Zhuravlyov, and N. A. Rybakova, 1994: Preliminary results of X-band polarization radar studies of clouds and precipitation. *J. Atmos. Oceanic Technol.*, **11**, 132–139.

Snyder, J. C., A. V. Ryzhkov, M. R. Kumjian, A. P. Khain, and J. Picca, 2015: A $Z_{DR}$ column detection algorithm to examine convective storm updrafts. *Wea. Forecasting*, **30**, 1819–1844.

Van Den Broeke, M. S., 2017: Polarimetric radar metrics related to tornado life cycles and intensity in supercell storms. *Mon. Wea. Rev.*, **145**, 3671–3686.

——, M. S., J. M. Straka, and E. N. Rasmussen, 2008: Polarimetric radar observations at low levels during tornado life cycles in a small sample of classic southern plains supercells. *J. Appl. Meteor. Climatol.*, **47**, 1232–1247.